BIOCHEMISTRY
including biophysical chemistry & molecular biology

Article

pubs.acs.org/biochemistry

Disability for Function: Loss of Ca^{2+}-Binding Is Obligatory for Fitness of Mammalian $\beta\gamma$-Crystallins

Shashi Kumar Suman,[†] Amita Mishra,[†] Lahari Yeramala, Ishan Das Rastogi, and Yogendra Sharma*

Centre for Cellular and Molecular Biology (CCMB), CSIR, Uppal Road, Hyderabad 500007, India

Supporting Information

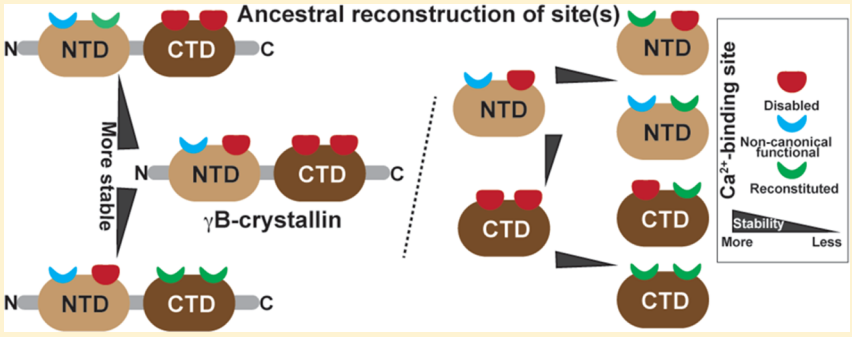

ABSTRACT: Vertebrate $\beta\gamma$-crystallins belonging to the $\beta\gamma$-crystallin superfamily lack functional Ca^{2+}-binding sites, while their microbial homologues do not; for example, three out of four sites in lens γ-crystallins are disabled. Such loss of Ca^{2+}-binding function in non-lens $\beta\gamma$-crystallins from mammals (e.g., AIM1 and Crybg3) raises the possibility of a trade-off in the evolutionary extinction of Ca^{2+}-binding. We test this hypothesis by reconstructing ancestral Ca^{2+}-binding motifs (transforming disabled motifs into the canonical ones) in the lens γB-crystallin by introducing minimal sets of mutations. Upon incorporation of serine at the fifth position in the N/D-N/D-X-X-S/T(5)-S motif, which endowed a domain with microbial characteristics, a decreased domain stability was observed. Ca^{2+} further destabilized the N-terminal domain (NTD) and its serine mutants profoundly, while the incorporation of a C-terminal domain (CTD) nullified this destabilization. On the other hand, Ca^{2+}-induced destabilization of the CTD was not rescued by the introduction of an NTD. Of note, only one out of four sites is functional in the NTD of γB-crystallins responsible for weak Ca^{2+} binding, but the deleterious effects of Ca^{2+} are overcome by introduction of a CTD. The rationale for the onset of cataracts by certain mutations, such as R77S, which have not been clarified by structural means, could be explained by this work. The findings presented here shed light on the evolutionary innovations in terms of the functional loss of Ca^{2+}-binding and acquisition of a bilobed domain, besides imparting additional advantages (e.g., protection from light) required for specialized functions.

$\beta\gamma$-Crystallins, which include eye lens $\beta\gamma$-crystallins, are an ever expanding superfamily with members spanning across various taxa ranging from microbes to vertebrates,[1−4] and thus are remarkable exemplars of the evolutionary diversification of new protein functions. The striking similarity in structures of lens $\beta\gamma$-crystallins with non-lens members, for example, $\beta\gamma$ domains of AIM1 and Crybg3 from higher vertebrates,[5−7] Ci-$\beta\gamma$-crystallin from *Ciona intestinalis*,[8] spherulin 3a (from a yeast), geodin (from a sponge) (both from lower eukaryotes),[9,10] and microbial (bacterial and archean) homologues,[11−18] is intriguing, despite the lack of much similarity at the amino acid sequence level. The major distinction between these evolutionarily related (from prokaryote and eukaryote including vertebrates) protein forms is the presence of canonical Ca^{2+}-binding motifs (i.e., N/D-N/D-X-X-S/T-S sequence) in proteins of microbial and lower eukaryotic origin,[9,17,18] which is lacking in the higher vertebrate homologues; most of the binding sites appear degenerated to the extent that Ca^{2+} binding is either very poor or lost.[9,19−21] The enigma of how ancestral forms of $\beta\gamma$-crystallins diverged into structurally similar microbial $\beta\gamma$-crystallins with Ca^{2+}-binding sites and lens, as well as nonlenticular homologues in vertebrates without Ca^{2+}-binding motifs, poses a challenging evolutionary puzzle. Based on the consensus sequence at the binding site, it is our forthright prediction that only one out of four sites of lens γB-crystallin would bind Ca^{2+} (for Ca^{2+}-binding scheme, Figure 1). This sole Ca^{2+}-binding site is responsible for weak Ca^{2+} binding noticed in lens β- and γ-crystallins, even as the functional consequences of such poor binding are not yet known.[21,22] However, it is speculated that at least in non-lenticular tissues (such as in brain and testes), these $\beta\gamma$-crystallins might be involved in hitherto unknown Ca^{2+}-dependent functions.[23,24]

Available data on Ca^{2+}-binding affinities to members of the $\beta\gamma$-crystallin superfamily reveal an interesting trend, which can be associated with the corresponding position of the members

Received: August 12, 2013
Revised: November 12, 2013
Published: November 19, 2013

 © 2013 American Chemical Society dx.doi.org/10.1021/bi401093n | *Biochemistry* 2013, 52, 9047−9058

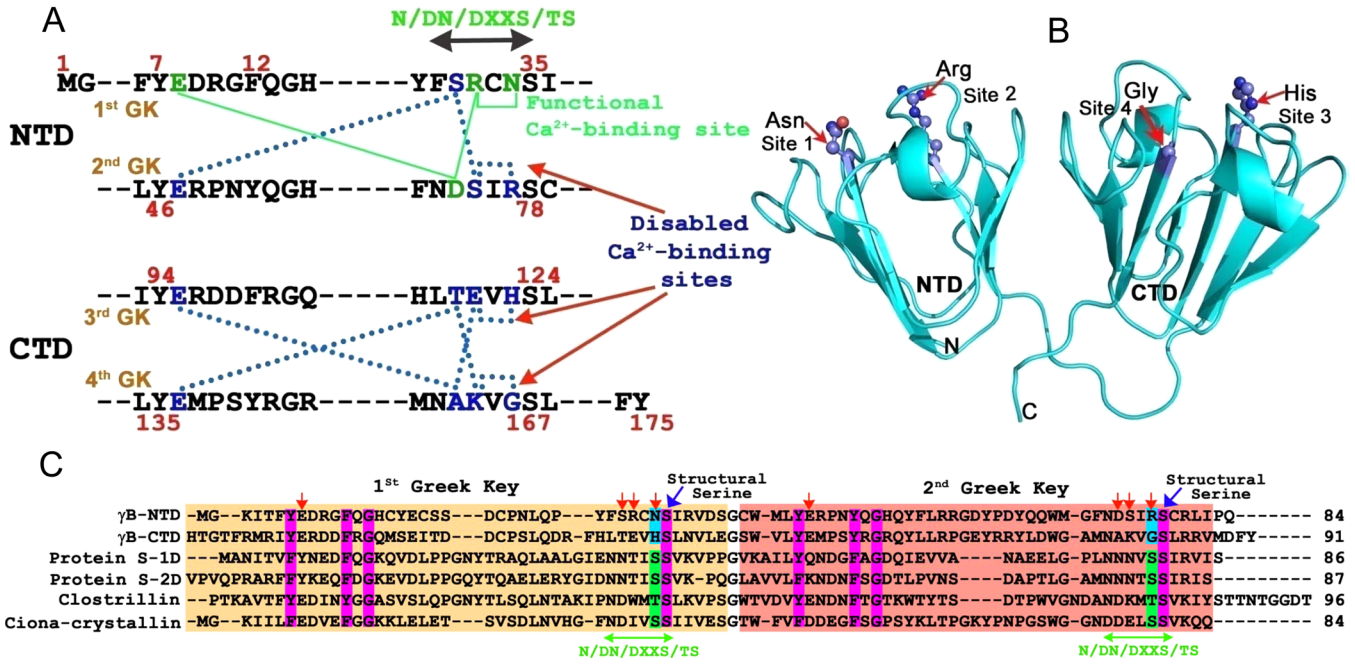

Figure 1. (A) Depiction of Ca^{2+}-binding motifs of the NTD and CTD of γ-crystallin based on the corresponding sequence of microbial relatives. Only one putative functional site is present in the N-terminal domain; the other three disabled sites of γB-crystallin are shown by solid green and dotted blue lines, respectively. (B) Position of the 5th residues, (corresponding to serine in microbial) of all four Ca^{2+}-binding sites is represented as ball and stick figures in the ribbon diagram of γB-crystallin crystal structure (PDB id 4GCR). (C) Sequence alignment of γB-crystallin with selected microbial relatives. The residues involved in Ca^{2+}-ligation are marked with red arrows. Conserved signature residues of βγ-crystallin-type Greek-key motifs are marked with purple boxes. The fifth serines of Ca^{2+}-binding motifs are highlighted in green in microbial crystallins. Serine is absent at this position in mammalian γB-crystallin (corresponding residues highlighted in cyan).

in existing evolutionary hierarchy with sound reasoning. While bacterial and archaeal members have higher affinity for Ca^{2+} (K_D for archaeal M-crystallin is 32 μM; bacterial members, protein S, 27 and 76 μM, and clostrillin, 5 μM),[12,17,25] members from lower eukaryotes have comparatively weaker binding affinity for the same (9 and 200 μM for spherulin 3a from slime mold, *Physarum polycephalum*).[26] The affinity is further decreased as one moves on to higher rungs of placement in the evolutionary ladder as seen in amphibian and mammalian members (260 μM for ep37 from amphibian, mammalian lens β- and γ-crystallins in the range of 200 μM),[17,20,21] thus suggesting a trend of diminished Ca^{2+}-binding.

The diversification of βγ-crystallins as Ca^{2+}-binders (in microbes and lower invertebrates) and poor or nonbinders (in higher vertebrates and mammals) puts up a remarkable query as to what was the evolutionary gain from the loss of Ca^{2+}-binding sites in βγ-crystallins of higher vertebrates. An approach to resolve and understand this may involve evolutionary reconstruction of lens γ-crystallins to their microbial forms. However, owing to high diversity in amino acid sequence, except conservation of a few signature residues, it is evidently unviable to convert a mammalian γ-crystallin to a microbial form even partially, if not in entirety. In the absence of a choice, we made use of the N/D-N/D-X-X-S/T-S Ca^{2+}-binding motif as a central scaffold for ancestral reconstruction in terms of Ca^{2+}-binding sites. Being conserved both in mammalian and in microbial βγ-crystallins, serine at the sixth (last) position in the motif sequence is a signature residue and is required for the proper domain fold.[3,11,27,28] While sixth serine does not participate directly in Ca^{2+} binding, this residue helps in delineating the corresponding motif in vertebrate crystallins. A detailed analysis of the Ca^{2+}-binding sequence brought the position and role of serine/threonine (at the fifth position) in the canonical (microbial) N/D-N/D-X-X-S/T-S motif to our notice. While this position is conserved and occupied by serine (and occasionally by threonine) in microbial members of this family, it varies in higher vertebrates (Figure 1). This fifth serine residue ligates Ca^{2+} via side chain coordination and is a critical determinant in ion binding,[8,9,17] because mutating this to arginine or lysine disables a site.[29] Other residues and their positions in Ca^{2+}-binding loops are more flexible and less consistent, thus the fifth serine remains the only choice. Therefore, substitution to serine at the fifth position of a disabled Ca^{2+}-binding motif partially converts a vertebrate-type degenerate Ca^{2+}-binding pocket to a microbial type, facilitating ancestral reconstruction of the motif for identification of novel properties for which Ca^{2+}-binding ability was traded off. A single mutation to serine would confer an increased microbial character to this motif without disturbing protein topology,[30] though restoring proper Ca^{2+} binding would also depend on the presence of other key residues in the binding loop.[17,29]

In this work, we manipulated mammalian lens γB-crystallin by inserting serine as the fifth residue in the corresponding Ca^{2+}-binding signature sequence of all four motifs. We report that while a mutation favoring Ca^{2+} binding in disabled motifs of γB-crystallin NTD decreases the stability of the domain, the situation is further exacerbated by Ca^{2+}, leading to a loss of stability of the manipulated domain. This is contrary to observations in other Ca^{2+}-binding proteins, including many microbial members of this superfamily, and perhaps is the only known case where Ca^{2+} binding destabilizes a protein domain. This acquired Ca^{2+}-induced instability of the NTD is nullified by the CTD in two-domain protein systems. Destabilization

dx.doi.org/10.1021/bi401093n | *Biochemistry* 2013, 52, 9047−9058

caused by serine replacement in the CTD by Ca^{2+} is not rescued by the NTD in a two-domain protein. We also present a comprehensible explanation as to why only a single Ca^{2+}-binding site in the N-terminal domain is functional, but none in the C-terminal domain. Our data strongly suggest that while Ca^{2+} binding might have been of vital need for ancestors of lens crystallins for their activities, most of the binding sites in lens $\beta\gamma$-crystallins were disabled to prevent Ca^{2+}-derived instability, thus providing a much sought explanation for cataractogenic mutations, which otherwise have not been understood structurally.[30]

MATERIALS AND METHODS

Cloning, Site-Directed Mutagenesis, Overexpression, and Purification of γB-Crystallin, Its Mutants, and Individual Domains. γB-Crystallin (175 amino acids) (accession number NP_001013612) from bovine (*Bos taurus*) lens was cloned in a pET-21a expression vector. Individual domains of γB-crystallin were separately amplified (1−75 as NTD and 76−175 as CTD) using specific sets of primers and cloned at *Nde*I and *Bam*HI sites in a pET21a expression vector. Specific mutations were introduced in full length as well as in individual domains by a PCR-based mutagenesis method. All recombinant plasmids were transformed into *E. coli* BL21-(DE3) cells and overexpression of proteins was induced by 1 mM IPTG at 18 °C for 14−16 h. The proteins were purified by ion-exchange chromatography on a SP-Sepharose column in 50 mM Bis-Tris buffer, pH 5.5, containing 1 mM DTT and 1 mM EDTA. The proteins were eluted by a linear gradient of 0 to 1.5 M NaCl, followed by gel filtration on a Superdex-75 column attached with a Bio-Rad Duo-Flow purification system.

Molecular Spectroscopy. Fluorescence emission spectra of proteins (0.1 mg/mL) were recorded on a F-4500 fluorescence spectrofluorimeter (Hitachi Inc., Japan) in 50 mM Tris-HCl, pH 7.0, and 100 mM KCl buffer at an excitation wavelength of 295 nm in correct spectrum mode of the instrument using excitation and emission bandpasses of 5 nm each. Surface hydrophobicity was monitored using bis-ANS (10 μM) as probe at 395 nm excitation, and emission spectra were recorded between 400 and 650 nm and corrected for equal concentrations of bis-ANS in buffer. Photolability of proteins (0.2 mg/mL) was analyzed by irradiating a solution at 280 nm (by setting excitation band-pass of 20 nm) and a change in tryptophan intensity was measured at 330 nm in time scan mode of the instrument (emission bandpass set at 2.5 nm).

Far- and near-UV circular dichroism (CD) spectra of proteins were recorded on a Jasco J-815 spectropolarimeter using 0.01 and 1 cm path length cuvettes, respectively. The spectra were corrected for buffer baseline. Effect of Ca^{2+} was monitored by titrating protein solutions in appropriate concentrations of standard calcium chloride solution (Fluka).

Isothermal Titration Calorimetry (ITC). Ca^{2+}-binding isotherms of proteins were determined on a Microcal VP-ITC (Microcal Inc., USA) as described earlier.[20] The protein solutions and calcium chloride (2−5 mM) were prepared in Chelex-treated 50 mM Tris, pH 7.0, and 100 mM KCl buffer. Protein solutions (1.4 mL, 100 μM) were used for the binding experiment at 30 °C. Aliquots of 2 μL of $CaCl_2$ as ligand solution were injected for each titration until saturation. Titration of the buffer with identical concentrations of $CaCl_2$ solution was also performed as blank. The fittings were performed using the software Origin (version 7.0) supplied by Microcal after subtraction with the appropriate buffer blank.

Thermal and GdmCl-Induced Protein Stability Analysis. Thermal unfolding was monitored by the change in ellipticity in far-UV range (215 nm for N-terminal domain and 218 nm for full length γB-crystallin) on a Jasco J-815 spectropolarimeter as a function of temperature between 25 and 85 °C using a Jasco peltier system attached to the sample holder at the rate of 1 °C/min. Data obtained were best fitted and plotted using Origin version 7.0.

Equilibrium unfolding induced by denaturant guanidinium chloride (GdmCl) was obtained by recording fluorescence emission spectra of proteins prepared in GdmCl in the range of 0−6 M concentration (total of 60 data points for each unfolding transition) in the apo (Ca^{2+}-free) and holo (Ca^{2+}-bound form) proteins. The ratios of fluorescence intensity (at 360/320 nm) were plotted as a function of GdmCl concentration by fitting to the following equation, which relates fluorescence intensity to the extent of unfolding. The equation used for two-state unfolding model:

$$Y_{obs} = \frac{\{Y_N + Y_u \exp(-(\Delta G_u^\circ - m1[D])/(RT))\}}{\{1 + \exp(-(\Delta G_u^\circ - m1[D])/(RT))\}}$$

The free energy of unfolding (ΔG_D) determined from the ratio of native to denatured protein at each GdmCl concentration was plotted against GdmCl concentration.[31] Fitness of a protein (based on change in stability due to a mutation, $\Delta\Delta G^{mt-wt}$) was expressed based on the change in the estimated free energy change of unfolding, which is defined as

$$\Delta\Delta G^{mt-wt} = \Delta G_{mutant} - \Delta G_{wt}$$

RESULTS

One of the observations is that lens β- and γ-crystallins, as well as non-lens βγ-crystallins (from mammals), such as AIM1 and Crybg3 do not have the canonical form of microbial-type N/D-N/D-X-X-S/T-S motif of Ca^{2+}-binding.[5,7] This peculiarity that microbial members generally have the Ca^{2+}-binding sites but the members of the higher taxa do not caught our attention, the basis of which we tried to figure out in this work.

Trade-Offs between Canonical and Disabled Ca^{2+}-Binding Sites in Lens γ-Crystallins. Ca^{2+} binds at the N/D-N/D-X-X-T/S-S motif generally present in microbial members,[9,17] there is no such clear motif in lens γ-crystallins. The four sequences of γB-crystallin corresponding to the Ca^{2+}-binding motif identified based on the conservation of the sixth serine signature are -FSRCNS- and -NDSIRS- in the first (NTD) domain and -LTEVHS- and -NAKVGS- in the second (CTD) domain (Figure 1). As seen in the analysis presented in Figure 1, site 1 (located in the NTD) has a propensity to bind Ca^{2+} albeit with weaker affinity due to the absence of serine at the fifth position (Ca^{2+} binding to lens γ-crystallins was demonstrated earlier using[45] $CaCl_2$ by the Hummel−Dreyer method of gel filtration).[21] Among the three sites, the second site on the NTD is a disabled site due to Arg77 in place of serine. Both sites in the CTD are highly degenerate (with no fingerprint) presenting an unambiguous case of a trade off between canonical and disabled sites during evolution.

Reconstruction of Ancestral Ca^{2+}-Binding Motifs in Lens γB-Crystallin by Serine Substitution. The key position for Ca^{2+} binding in microbial relatives occupied by a serine at the fifth position (in N/D-N/D-X-X-T/S-S motif) is occupied by Asn34, Arg77, His123, and Gly166 in all four binding loops in lens γB-crystallin. As part of ancestral

dx.doi.org/10.1021/bi401093n | *Biochemistry* 2013, 52, 9047−9058

Table 1. Mutational Strategy for Reconstruction of Disabled Ca^{2+}-Binding Sites of γB-Crystallin to Microbial-Type[a]

MGKITFYEDRGFQGHCYECSSDCPNLQPY**FSRCNS**IRVDSGCWMLYERPNYQGHQYFLRRGDYPDYQQ
WMGF**NDSIRS**CRLIPQHTGTFRMRIYERDDFRGQMSEITDDCPSLQDRFH**LTEVHS**LNVLEGSWVLYE
MPSYRGRQYLLRPGEYRRYLDWGAM**NAKVGS**LRRVMDFY

N-terminal domain (NTD)		
Wild Type	FSRCNS------NDSIRS	
N34S	FSRCSS------NDSIRS	Ser at 1^{st} site in place of 5^{th} Asn
R77S	FSRCNS------NDSISS	Ser at 2^{nd} site in place of 5^{th} Arg
N34S,R77S	FSRCSS------NDSISS	Ser at both sites
C-terminal domain (CTD)		
Wild Type	LTEVHS------NAKVGS	
H123S	LTEVSS------NAKVGS	Ser at 1^{st} site in place of 5^{th} His
G166S	LTEVHS------NAKVSS	Ser at 2^{nd} site in place of 5^{th} Gly
H123S,G166S	LTEVSS------NAKVSS	Ser at both sites
γB-crystallin (Full length)		
Wild Type	FSRCNS------NDSIRS----LTEVHS------NAKVGS	
N34S	FSRCSS------NDSIRS----LTEVHS------NAKVGS	
R77S	FSRCNS------NDSISS----LTEVHS------NAKVGS	
N34S,R77S	FSRCSS------NDSISS----LTEVHS------NAKVGS	
H123S	FSRCNS------NDSIRS----LTEVSS------NAKVGS	
G166S	FSRCNS------NDSIRS----LTEVHS------NAKVSS	
N34S,R77S,G166S	FSRCSS------NDSISS----LTEVHS------NAKVSS	

[a]Underlined blue colored sequence refers to CTD. Substituted residue(s) marked shown in red with respect their wt protein. Representative six residue stretch (Ca^{2+}-binding motif) of NTD and CTD are depicted in black and blue, respectively.

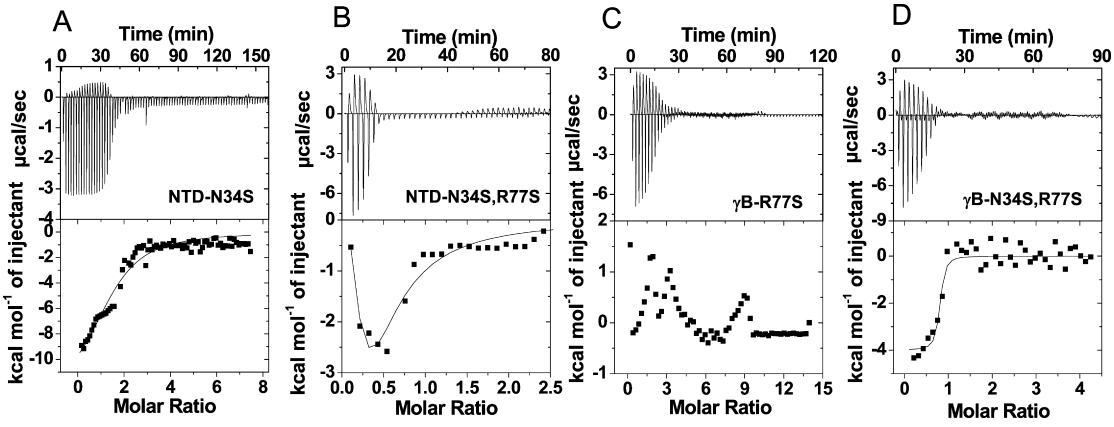

Figure 2. ITC thermograms of Ca^{2+} binding to NTD, (A) N34S, (B) N34S/R77S mutants, and to the two-domains, (C) R77S, (D) N34S/R77S mutants, of γB-crystallin. Only NTD-N34S and its double mutant show measurable heat changes (NTD-R77S does not show heat change as also reported earlier (see ref 20). Mutants R77S and N34S/R77S of the two-domain protein showed heat changes during Ca^{2+} titration. Data could not be fitted in case of the R77S mutant of two-domain protein.

reconstruction of γB-crystallin, mutations were created in each motif by replacing these residues with serine, which are thus expected to confer microbial features. The mutants created were N34S, R77S (also referred to as Ser1 and Ser2) and a double mutant N34S/R77S in the NTD of γB-crystallin. Similarly, mutants H123S, G166S (referred to as Ser3 and Ser4), and H123S/G166S (double mutant) were created in the CTD. Individual NTDs and CTDs with the above-mentioned mutations were also prepared as corresponding controls (Table 1).

Ca^{2+}-Binding Energetics. Study of Ca^{2+}-binding to NTD as well as to two-domains and their serine mutants was attempted by ITC (Figure 2). Owing to weak affinity, isotherms of Ca^{2+}-binding to γB-crystallin and its mutants did not fit well as seen in the case of other Ca^{2+}-binding proteins (such as those of the EF-hand family of proteins). Significantly, we still see that both R77S and double mutants (R77S/N34S) of the two-domain protein demonstrated measurable heat changes upon Ca^{2+} titration (Figure 2), but only the data obtained with double mutants could be evaluated by fitting (data not suitable for fitting in the case of γB-crystallin R77S mutant). We did not notice heat change of Ca^{2+} binding by ITC to the NTD and its NTD-R77S mutant (confirming our earlier observations).[20] Ca^{2+} binding to NTD-N34S and double mutant was driven by favorable enthalpy and unfavorable entropy (Table S1, Supporting Information). The apparent dissociation constants of Ca^{2+}-binding to NTD-N34S and double mutants were 29 and 19 μM respectively, while it was 45 μM for the double mutant (R77S/N34S) of the two-domain protein. These ITC results demonstrate Ca^{2+} binding to γB-crystallin and certain mutants unambiguously, though deducing

dx.doi.org/10.1021/bi401093n | Biochemistry 2013, 52, 9047−9058

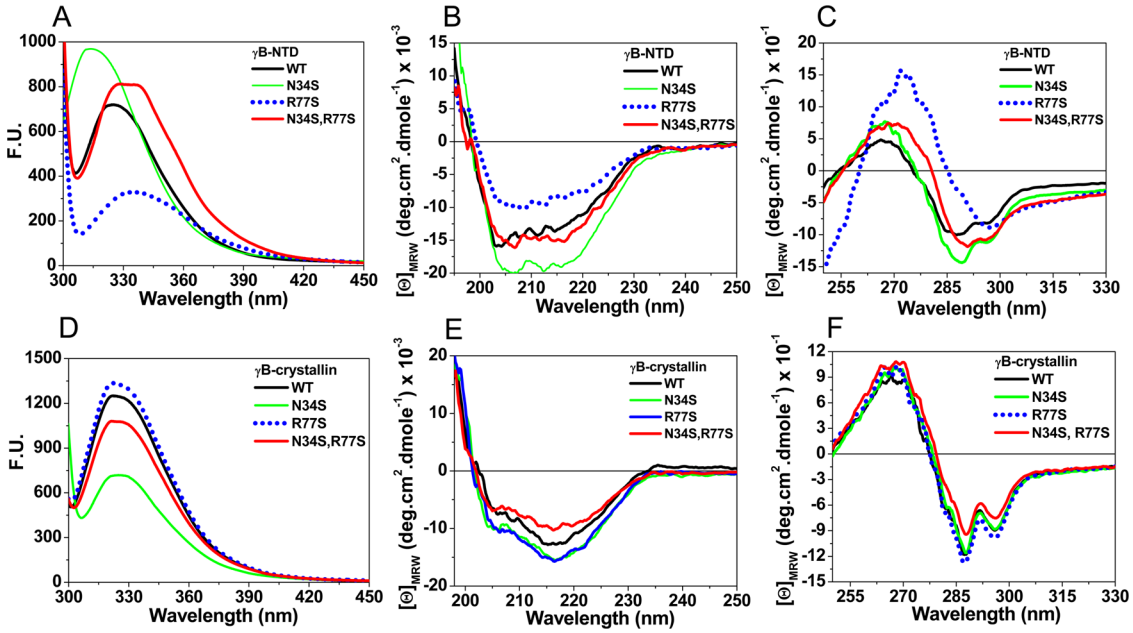

Figure 3. Conformational features of the NTD and two-domain γB-crystallin. Intrinsic trytophan fluorescence (A, D); far-UV CD (B, E), and near-UV CD (C, F) spectra of the NTD and two-domain protein. Specific mutations were incorporated only in the Ca^{2+}-binding sites of the NTD.

Table 2. Thermodynamic Parameters Deduced from Chemical Unfolding and Temperature Midpoint of the N-Terminal Domain of γB-Crystallin and Its Mutants

	$\Delta G°$ kcal mol^{-1}		m kcal mol^{-1} M^{-1}		$c_{1/2}$ [M]		
protein	EDTA	$CaCl_2$	EDTA	$CaCl_2$	EDTA	$CaCl_2$	T_m (°C)
			NTD				
WT	8.5 ± 0.22	6.3 ± 0.23	2.7 ± 0.07	2.4 ± 0.09	3.1 ± 0.10	2.5 ± 0.12	78.3
N34S	7.4 ± 0.23	6.2 ± 0.37	2.4 ± 0.07	2.9 ± 0.17	2.9 ± 0.10	2.0 ± 0.15	71.4
R77S	2.6 ± 0.13	2.2 ± 0.07	1.1 ± 0.05	1.0 ± 0.03	2.3 ± 0.16	2.0 ± 0.12	65.0
N34S/R77S	7.1 ± 0.20	5.4 ± 0.27	2.3 ± 0.06	2.4 ± 0.12	3.0 ± 0.11	2.2 ± 0.09	70.0
			Two-Domain				
WT	10.8 ± 0.34	10.8 ± 0.40	3.4 ± 0.10	3.5 ± 0.13	3.1 ± 0.10	3.0 ± 0.08	79.8
N34S	11.5 ± 0.62	8.9 ± 0.32	3.9 ± 0.21	3.2 ± 0.11	2.9 ± 0.13	2.8 ± 0.10	78.9
R77S	9.7 ± 0.23	10.5 ± 0.38	3.0 ± 0.07	3.4 ± 0.12	3.2 ± 0.10	3.0 ± 0.12	80.1
N34S/R77S	9.0 ± 0.23	8.8 ± 0.25	3.0 ± 0.07	3.1 ± 0.1	3.0 ± 0.07	2.8 ± 0.10	77.8

a dissociation constant was not possible due to the nature of the isotherm in R77S mutant.

Conformational Effects of Ancestral Reconstruction on NTD. We observed significant consequences of serine substitution on NTD conformation but not on the two-domain protein. Ser1 (N34S) caused a blue shift in tryptophan fluorescence (~8 nm, from 328 to 320 nm) and increased ellipticity in far-UV CD, while Ser2 (R77S) resulted in a red shift of ~7 nm with a decreased ellipticity, thus disturbing the conformation. Substituting Ser1 and Ser2 (N34S/R77S) in both the Ca^{2+}-binding motifs (double mutant) resulted in a broad emission peak, and minor changes in secondary but significant changes in tertiary conformations were seen. These conformational settings conferred by Ser1 and Ser2 replacements in the NTD were nullified by the CTD in the two-domain protein. In other words, no such conformational deformity by these mutations was observed in protein with both domains (Figure 3). These results suggest that the conformational changes caused by serine in the NTD are neutralized by the CTD. On the other hand, such conformational changes in the CTD by serine substitution were comparatively less pronounced and were not corrected by the NTD (see below). Serine substitution decreases thermal stability of the NTD (T_m decreases by 8−10 °C), while there is no such change noticed in stability of the two-domain protein (Figure 3 and Table 2). The NTD and its serine mutants form dimers in solution, with a more flexible conformation of NTD-R77S (asymmetric elution peak) under the conditions tested (Figure S1, Supporting Information). The R77S mutation leads to a greater exposure of hydrophobic regions compared with WT and other mutants as seen by higher intensity of Bis-ANS fluorescence (Figure S1, Supporting Information). In case of the two-domain protein and its serine mutants, only the N34S mutant showed higher bis-ANS fluorescence (Figure S1, Supporting Information).

Unanticipated Destabilization of NTD by Ca^{2+}. Equilibrium unfolding of the NTD and its serine mutants (N34S, R77S, and double mutant N34S/R77S) was performed in the presence or absence of Ca^{2+} (Figure 4). Unexpectedly, in the presence of Ca^{2+}, the NTD undergoes significant destabilization as seen by $\Delta\Delta G^{holo-apo} \approx -2.2$ kcal/mol, rather than stabilization ($c_{1/2,apo}$ = 3.1 M, ΔG = 8.5 kcal/mol to $c_{1/2,holo}$ = 2.5 M, ΔG = 6.3 kcal/mol). The conformational stability of apo NTD-N34S mutant ($c_{1/2}$ = 2.9 M, ΔG = 7.4 kcal/mol) was

dx.doi.org/10.1021/bi401093n | Biochemistry 2013, 52, 9047−9058

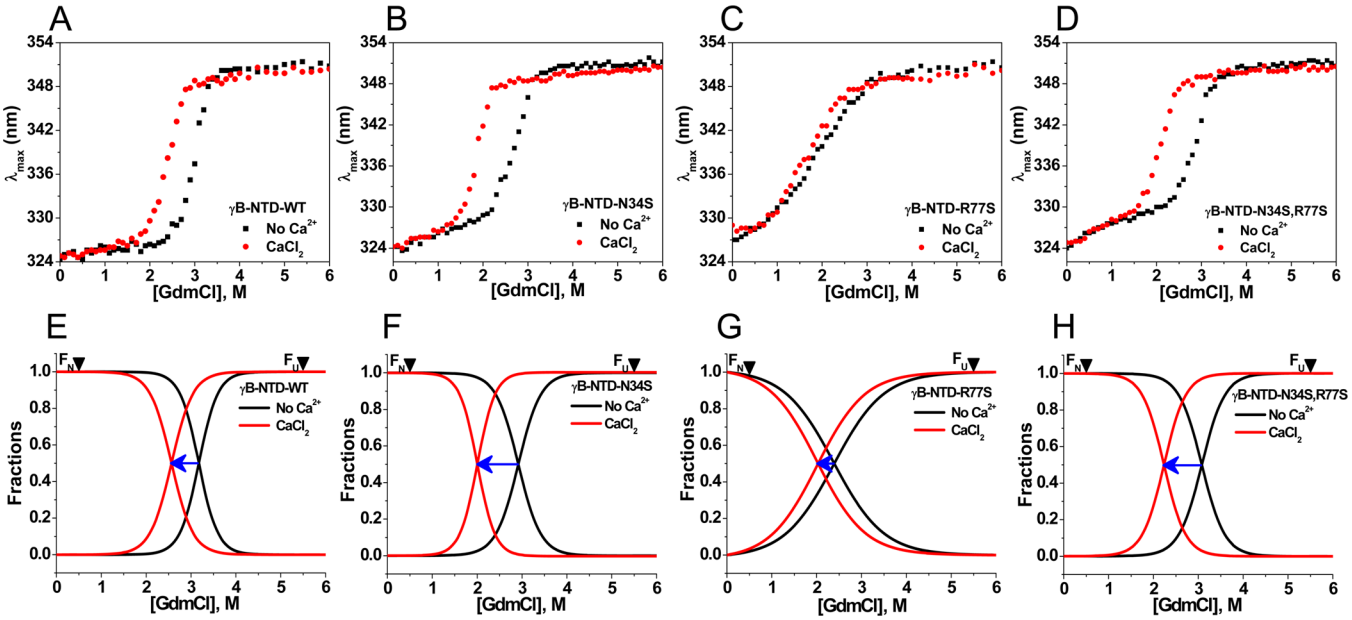

Figure 4. Ca^{2+} destabilizes the NTD and its serine mutants. Tryptophan fluorescence emission maxima of the NTD plotted with GdmCl concentrations: (A) WT, (B) N34S, (C) R77S, and (D) N34S/R77S mutants. Best fit of the fractions of (E) WT, (F) N34S, (G) R77S, and (H) N34S/R77S mutants with GdmCl concentration. Unfolding was followed in Ca^{2+} free state (with 1 mM EDTA) or in the presence of 5 mM $CaCl_2$. Inherent protein stability of NTD is significantly compromised due to R77S mutant. F_N and F_U denote fractions of native and unfolded states. Data were best fit to a two-state model of unfolding.

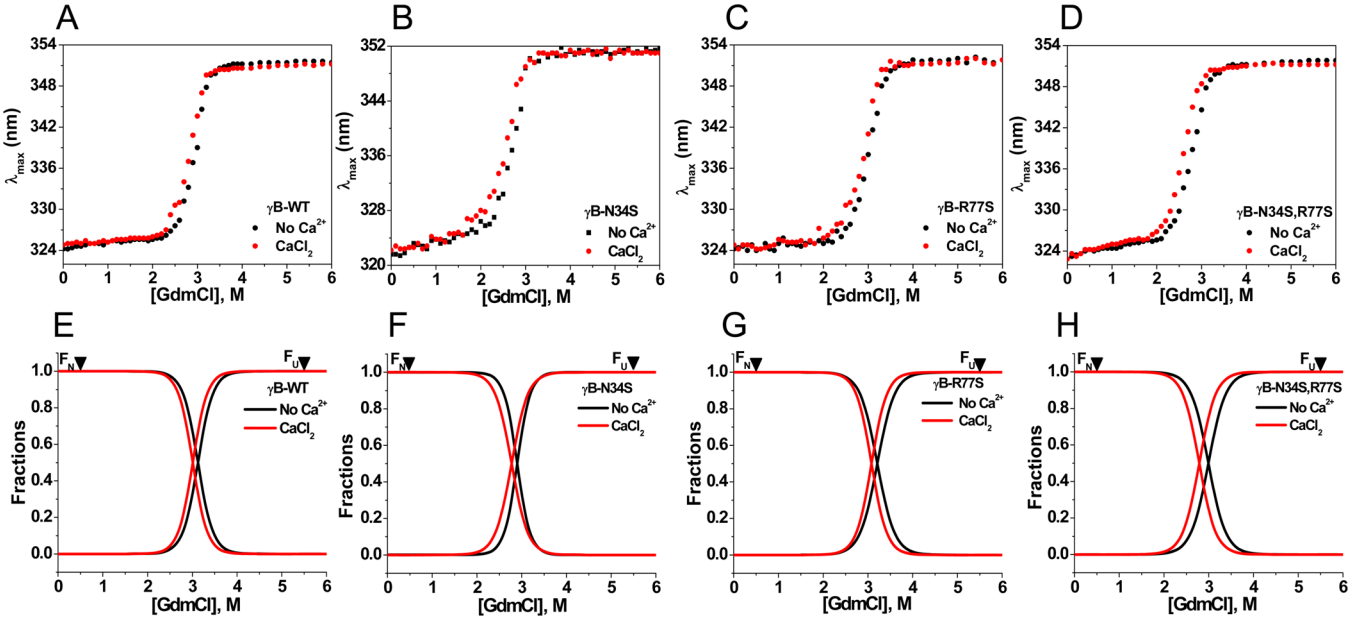

Figure 5. Domain stability of γB-crystallin after ancestral reconstruction of Ca^{2+}-binding sites in the NTD. Intrinsic tryptophan fluorescence wavelength emission maxima of two-domain (A) WT, (B) N34S, (C) R77S, and (D) N34S/R77S mutants as a function of GdmCl concentration. Best fit of the fractions of (E) WT, (F) N34S, (G) R77S, and (H) N34S/R77S mutants as a function of GdmCl concentration. Unfolding was followed in Ca^{2+} free state (with 1 mM EDTA) or in the presence of $CaCl_2$ (5 mM). Data were best fit to a two-state model of unfolding. Ca^{2+}-induced destabilization was not seen in any mutants of the two-domain protein.

comparable to its WT ($c_{1/2}$ = 3.1 M, ΔG = 8.5 kcal/mol) except in the slope before transition state (Figure 4 and Table 2).

Ca^{2+} significantly reduced the stability of NTD-N34S ($c_{1/2}$ = 2.0 M, ΔG = 6.2 kcal/mol) compared with its apo form, demonstrating destabilization of the domain by Ca^{2+}. Of note, a drastically lower stability for NTD-R77S ($c_{1/2}$ = 2.3 M, ΔG = 2.6 kcal/mol) in comparison with the WT ($c_{1/2}$ = 3.1 M, ΔG = 8.5 kcal/mol) was observed ($\Delta\Delta G^{mt-wt} \approx -5.9$ kcal/mol), which is rather a higher $\Delta\Delta G$ value, which defines fitness due to a mutation (a protein would be more disabled if $\Delta\Delta G$ is >3 kcal/mol).[32] This mutant follows slow unfolding even at low concentrations of GdmCl (<0.5 M). In this case, only a noticeable reduction in domain stability was observed with Ca^{2+} ($c_{1/2}$ = 2.0 M, ΔG = 2.2 kcal/mol) compared with apo NTD-R77S (Figure 4 and Table 2). However, substitution of serine at both the sites (double mutant; N34S/R77S) did not affect

dx.doi.org/10.1021/bi401093n | Biochemistry 2013, 52, 9047−9058

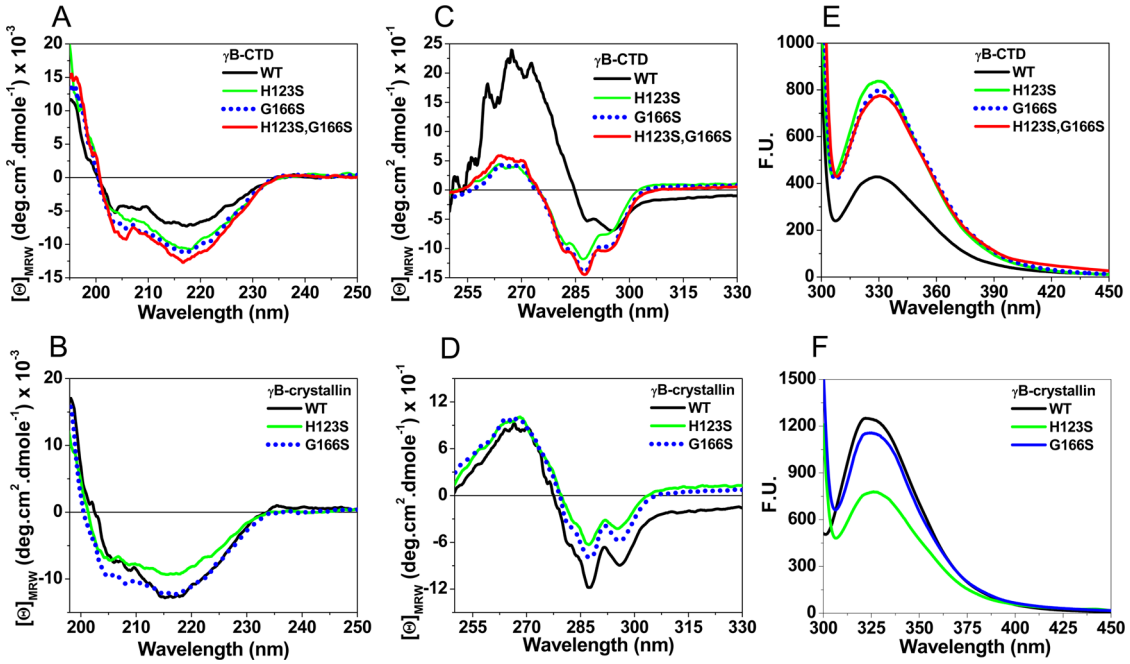

Figure 6. Conformational features of the CTD and two-domain γB-crystallin: (A, B) far-UV CD; (C, D) near-UV CD; (E, F) tryptophan fluorescence. Specific mutation was incorporated only in Ca^{2+}-binding sites of the CTD.

Table 3. Thermodynamic Parameters Deduced from Chemical Unfolding and Temperature Midpoint of the C-Terminal Domain of γB-Crystallin and Its Mutants

	$\Delta G°$ kcal mol^{-1}		m kcal mol^{-1} M^{-1}		$c_{1/2}$ [M]		
protein	EDTA	$CaCl_2$	EDTA	$CaCl_2$	EDTA	$CaCl_2$	T_m (°C)
			CTD				
WT	6.4 ± 0.21	6.6 ± 0.26	3.0 ± 0.10	3.1 ± 0.12	2.1 ± 0.10	2.1 ± 0.11	61.0
H123S	5.2 ± 0.26	5.2 ± 0.27	2.8 ± 0.13	2.8 ± 0.14	1.8 ± 0.07	1.8 ± 0.08	62.5
G166S	4.4 ± 0.27	4.2 ± 0.26	2.7 ± 0.16	2.6 ± 0.15	1.6 ± 0.12	1.6 ± 0.09	62.5
H123S/G166S	5.2 ± 0.26	4.1 ± 0.26	2.8 ± 0.13	2.5 ± 0.15	1.9 ± 0.10	1.6 ± 0.08	61.6
			Two-Domain				
H123S	5.3 ± 0.18	6.4 ± 0.23	1.7 ± 0.06	2.2 ± 0.08	2.8 ± 0.08	2.4 ± 0.06	76.7
G166S	5.7 ± 0.14	6.5 ± 0.26	1.9 ± 0.05	2.4 ± 0.10	2.9 ± 0.10	2.5 ± 0.08	74.6
N34S/R77S/G166S	5.0 ± 0.15	6.4 ± 0.70	1.9 ± 0.06	2.7 ± 0.33	2.5 ± 0.12	2.0 ± 0.11	70.9

stability of the apo form substantially (fitness $\Delta\Delta G^{mt-wt} \approx -1.7$ kcal/mol, $c_{1/2}$ = 3.0 M, ΔG 7.1 kcal/mol) suggesting that the first motif endured the effect of serine replacement compared with the second motif. Ca^{2+} also destabilized the double mutant (NTD-N34S/R77S) ($c_{1/2}$ =2.2 M, ΔG = 5.4 kcal/mol, $\Delta\Delta G^{holo-apo} \approx -1.7$ kcal/mol) (Figure 4 and Table 2). Ca^{2+} induces conformational changes only in NTD double mutants as noticed by near-UV CD spectra, while the NTD and its serine mutants showed quenched fluorescence upon Ca^{2+} titration.

CTD Nullifies Destabilization of NTD by Ca^{2+}. Equilibrium unfolding of serine mutations (in the NTD) of two-domain γB-crystallin (N34S, R77S, and double mutant N34S/R77S) was performed to assess the role of the CTD in influencing the effect of mutations in the NTD (Figure 5 and Table 2).

No significant change in conformational stability due to serine mutations (in the NTD) of the two-domain protein was noticed as indicated by similar $c_{1/2}$ values (Table 2). Conformational stability of the NTD (described in terms of $c_{1/2}$ = 3.1 M) was similar to that of two-domain protein ($c_{1/2}$ = 3.1 M) (Figure 5 and Table 2). In contrast to the NTD, there was negligible Ca^{2+}-induced destabilization of the two-domain protein carrying serine mutations in the NTD (Figure 5 and Table 2). These results suggest that the presence of the CTD as a second domain in γ-crystallins plays a controlling role in neutralizing the Ca^{2+}-induced destabilization that is imposed on the NTD. In an evolutionary context, the undermining effects of Ca^{2+} on the structural robustness of the NTD were nullified by the CTD, which implies that during evolution not only a domain with enhanced stability was created by trading off the Ca^{2+}-binding ability, but also another domain was incorporated. Thus, γ-crystallin evolved as a two-domain protein, which also acquired additional advantages, such as protection of labile tryptophan residues against UV light.[33]

Conformational Changes in the CTD by Ancestral Reconstruction But No Destabilization by Ca^{2+}. Both Ca^{2+}-binding loops of the CTD are extensively modified. Similar to the NTD, substitution of His123 and Gly166 by serine residues in the CTD would endow ancestral characters through manipulation of disabled Ca^{2+}-binding motifs. In contrast to the NTD, however, all the three CTD serine mutants (H123S, G166S and double mutant H123S/G166S) showed enhanced ellipticity in far-UV CD as well as

dx.doi.org/10.1021/bi401093n | Biochemistry 2013, 52, 9047−9058

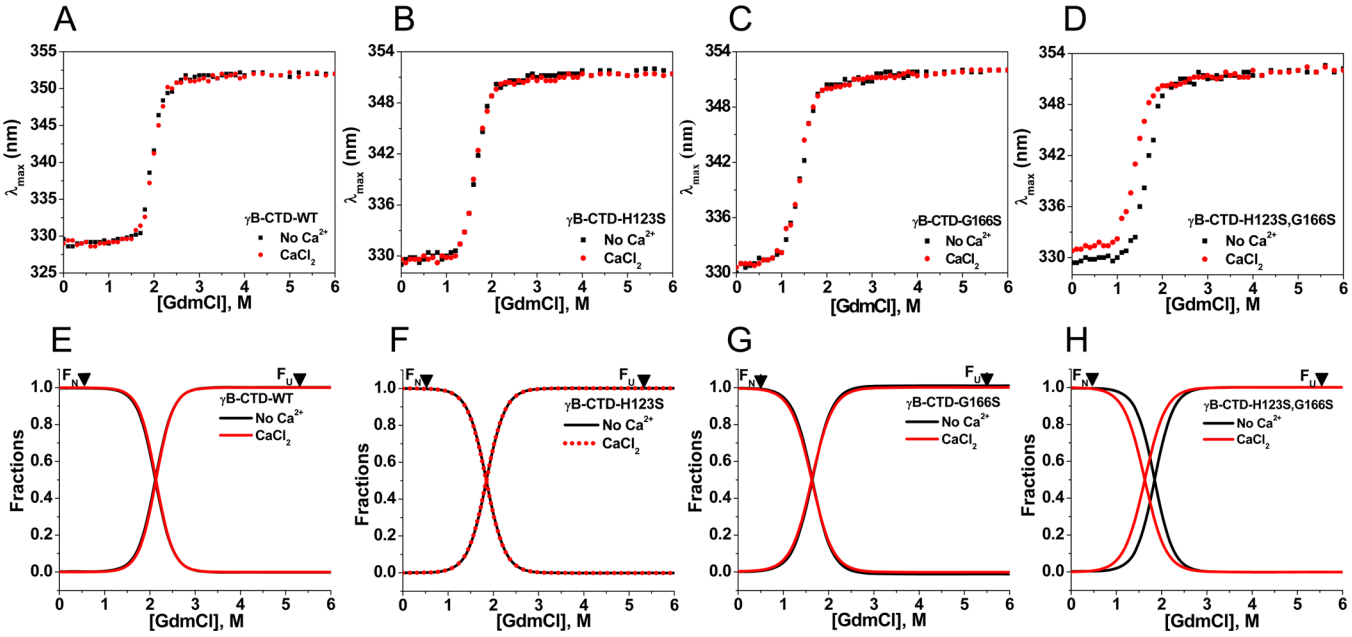

Figure 7. Alteration in domain stability of the CTD of γB-crystallin after ancestral reconstruction of Ca^{2+}-binding motifs. Tryptophan fluorescence emission maxima of CTD: (A) WT, (B) H123S, (C) G166S, and (D) H123S/G166S mutants with GdmCl concentrations. Best fit of the fractions of (A) WT, (B) H123S, (C) G166S, and (D) H123S/G166S mutants with GdmCl concentrations. Unfolding was followed either in the presence or in the absence of $CaCl_2$.

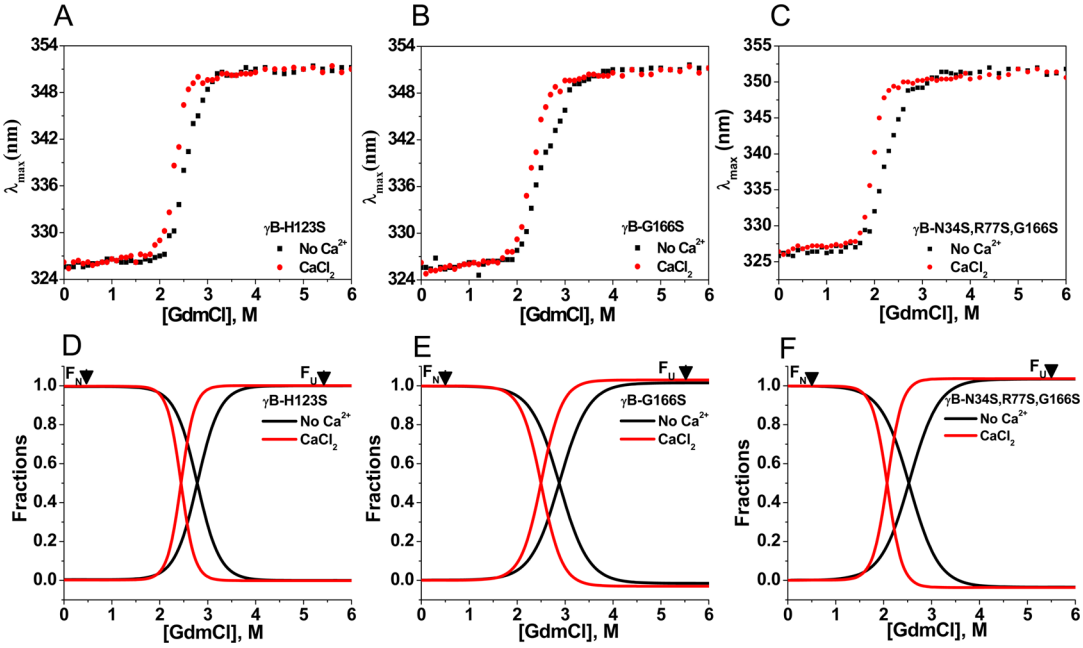

Figure 8. Domain stability of γB-crystallin after ancestral reconstruction of Ca^{2+}-binding motifs of the CTD. Tryptophan fluorescence λ_{max} of two-domain (A) H123S, (B) G166S, and (C) N34S/R77S/H123S mutants as a function of GdmCl concentration represented. Best fit of the fractions of (D) H123S, (E) G166S, and (F) N34S/R77S/H123S mutants as a function of GdmCl concentration are shown. Ca^{2+} destabilizes all the mutants.

fluorescence intensity compared with the WT (Figure 6). Emission maxima (λ_{max}) of WT and serine mutants of the CTD (~330 nm) were red-shifted in comparison to serine mutants of the NTD, suggesting a disturbance in the tryptophan microenvironment. Serine substitution (H123S/G166S) in both the loops results in insignificant changes in secondary and tertiary conformations. There is no alteration in thermal stability of the CTD by these serine mutations (Table 3). The CTD itself is less thermally stable than the NTD, and unlike in the case of NTD mutants, serine substitution had no effect on the stability of the CTD (Table 3). These results demonstrate that these mutations in the CTD are comparatively more tolerable than in the NTD, because serine substitution does not affect domain properties as severely as in the case of the NTD.

The conformational stability of the CTD ($c_{1/2}$ = 2.1 M, ΔG = 6.4 kcal/mol) is less than that of its sister NTD ($c_{1/2}$ = 3.1 M, ΔG = 8.5 kcal/mol, $\Delta\Delta G^{CTD-NTD} \approx -2.1$ kcal/mol). Equilibrium unfolding of the CTD and its serine mutants showed that intrinsic conformational stability was compromised but unlike the NTD, it was independent of the presence of Ca^{2+}

dx.doi.org/10.1021/bi401093n | Biochemistry 2013, 52, 9047−9058

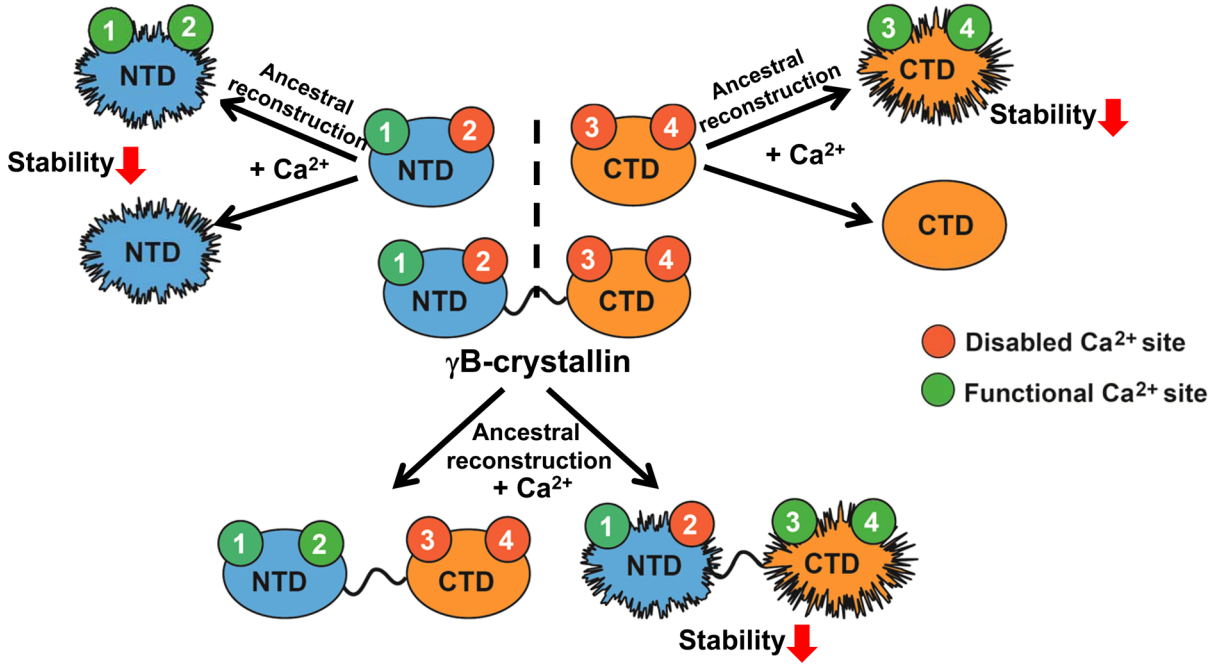

Figure 9. Schematic representation of Ca^{2+}-mediated effects on individual as well as on two-domain γB-crystallin. Ancestral subfunction, that is, restoration of Ca^{2+} binding, results in compromised domain stability as seen in individual domains of the NTD and CTD, depicted as distorted blue and orange ovular shapes, shown in the upper panel. Recruitment of a CTD could not add any additional stability to γ-crystallins but rectified the adverse effects on stability caused by Ca^{2+}, depicted in the lower panel. The NTD alone is unable to do the same, caused by Ca^{2+}. Green and red circles depict the functional and disabled Ca^{2+}-binding sites. Distorted oval shapes depict the reduction in stability, while the firm oval shape represents no effect in domain stabilities of γB-crystallin.

(Figure 7 and Table 3). The presence of Ca^{2+} destabilized partially only the double mutant of CTD-H123S/G166S (apo $c_{1/2}$ = 1.9 M, ΔG = 5.2 kcal/mol; holo $c_{1/2}$ = 1.6 M, ΔG = 4.1 kcal/mol, a moderate $\Delta\Delta G^{holo-apo} \approx -1.1$ kcal/mol) (Figure 7 and Table 3). A single serine replacement in either site of the CTD attenuated inherent stability ($\Delta\Delta G^{mt-wt} \approx -5.8$ kcal/mol) only, while Ca^{2+}-induced destabilization was noticed only in the double mutant of CTD (Table 3).

The NTD Is Unable to Rectify Ca^{2+}-Induced Destabilization in Two-Domain Crystallin That Carries Ancestral Ca^{2+}-Binding Motifs in the CTD (Serine Mutants). As noticed above, the NTD and its serine mutants showed significant Ca^{2+}-induced destabilization, which was nullified in the two-domain protein. On the other hand, serine incorporated in the CTD in two-domain γB-crystallin showed distinct destabilization induced by Ca^{2+} (Figure 8 and Table 3). The stability of γB-crystallin mutants H123S ($c_{1/2}$ = 2.8 M) and G166S ($c_{1/2}$ = 2.9 M) was comparable to that of WT ($c_{1/2}$ = 3.1 M) but stabilities of both mutants were reduced significantly in the presence of Ca^{2+} ($c_{1/2,holo}$ = 2.4 M), suggesting considerable destabilization even of the two-domain protein (Table 3). A triple serine mutant (N34S/R77S/H123S) of the two-domain protein showed inherent as well as Ca^{2+} induced destabilization (Figure 8 and Table 3).

These studies suggest that a weaker CTD (compromised domain stability due to serine mutations) was inefficient in controlling the adverse effect of mutations and Ca^{2+} in the two-domain protein. The NTD is somewhat more stable than the CTD but is weaker in the presence of Ca^{2+}. The CTD does not let the protein get destabilized by Ca^{2+} and thus rectifies the destabilizing effects of a weaker sister domain (NTD). This interdomain communication between the NTD and the CTD of γ-crystallins enables the protein to prevail as an intrinsically stable, long-lived protein suited for functioning as a lens protein.

DISCUSSION

As described in the introduction section, a decreasing trend of Ca^{2+}-binding affinity can be related to evolution, where it is reduced as one moves on to higher rungs of placement in evolutionary ladder. We thus propose an inversely proportional relationship between Ca^{2+} affinity and the placement of the members in evolutionary order. Absence of typical Ca^{2+}-binding sites in βγ-crystallins of higher vertebrates but presence in their microbial homologues makes us wonder about the factors that effected this loss of ability, providing a classic example of a protein subset displaying evolutionary loss of Ca^{2+}-binding functions. This appears to be the first known case where prospective Ca^{2+}-binding proteins were rendered as very poor or almost non-Ca^{2+}-binders during recruitment for a specific purpose, not only in lens but also in multiple non-lens protein members from higher vertebrates (two known examples being AIM1 and Crybg3).[5,7,34] Here, we have attempted to rationalize the evolutionary obligations implicated through experiments involving the manipulation of the Ca^{2+}-binding loops. Our results demonstrate that the inability of motifs to bind Ca^{2+}, particularly in the CTD, and only a weak site in the NTD are evolutionary compulsions from its ancestors that had canonical Ca^{2+}-binding sites. The available data reveal a decreasing affinity gradient of Ca^{2+} binding during evolution, followed by a sudden loss of binding. The first site (located in the NTD) is apparently responsible for the weak Ca^{2+} affinity to γ-crystallins (Figure 1).[21] If γ-crystallins had evolved as a single-domain NTD type protein (this supposition is also based on the fact that its nearest known precursor or ancestor Ci-βγ-crystallin (from *Ciona intestinalis*) is a one-domain protein but

dx.doi.org/10.1021/bi401093n | *Biochemistry* 2013, 52, 9047−9058

with canonical Ca^{2+}-binding sites),[8] Ca^{2+} would destabilize the protein, questioning its adaptability to be a lens crystallin. Decreased ability for Ca^{2+} binding was selected to increase the inherent stability of a domain; thus, three out of four sites became disabled during evolution (Figure 1). Ca^{2+} binding was traded off for a CTD to compensate Ca^{2+}-dependent destabilization and also for overall domain stability. Therefore, it was a functional compulsion to have a CTD which also provided additional advantages, because interdomain pairing also protects crucial tryptophan residues from photo-oxidation that may lead to destabilization of γ-crystallins.[33,35,36]

It has not been possible to monitor Ca^{2+} binding to wt γ-crystallin by ITC owing to a weak affinity site for ion binding, which is not strange. We see the measurable heat change only if there are specific mutations in the binding sites conferring microbial characters. These ITC data, though not well fit, are more significant in demonstrating clearly the Ca^{2+} binding ability of the mutants, particularly when Ca^{2+} binding to wt protein could not be monitored by ITC. Our data provide explanations as to why the CTD does not have any functional Ca^{2+}-binding site. Based on the reasoning presented here, we suggest that if there were a functional site in the CTD, the NTD would not nullify Ca^{2+}-dependent destabilization. Specifically, we provide explanations to (i) why there is a functional site in the NTD only and not in CTD and (ii) what were the compulsions to have a CTD for evolving lens γ-crystallins as a two-domain protein (Figure 9)? We believe that this serine residue (the fifth residue of the Ca^{2+}-binding motif) located in the loop region was an important spot for evolutionary requirements because it dictates a domain's physicochemical and consequently interdomain pairing properties (such as stability),[20] interestingly without disturbing domain topology, as shown in the case of cataract causing R77S mutation of γ-crystallin.[30,37]

For a long time, proper intracellular Ca^{2+} homeostasis in lens fiber cells has been documented to be critical for lens transparency because any disturbance in Ca^{2+} level is implicated in lens opacification or cataracts.[38−42] The disturbed Ca^{2+} level possibly causes the activation of Ca^{2+}-dependent calpains and transglutaminases, connexins, or aquaporins (only a few references are cited).[43−46] Some mutations in Ca^{2+}-binding loops, such as R77S, cause γ-crystallin to show measurable heat changes upon Ca^{2+} binding. Undoubtedly, this acquired Ca^{2+} binding would lead to a disturbance in intracellular Ca^{2+} homeostasis in lens fiber cells. Comparatively higher vulnerability of R77S mutant to photodamage (data presented in Figure S2, Supporting Information) substantiates its involvement in the onset of cataract, which may be explained by the alterations in ion-binding properties. Our study suggests that the disturbance in lens Ca^{2+} homeostasis due to the acquired Ca^{2+} binding of R77S mutated γD-crystallin is a strong reason for the loss of lens transparency.

It is recognized that flexible loop regions are hotspots in ancestrally related proteins for evolutionary modifications. Incidentally, this serine replacement (more prominent by serine of second Greek key motif) affects the hydrophobic core as seen by decreased "*m*" values (Table 2 and Table 3), which is essential for stability of γ-crystallins.[35] Inherent stability of lens γ-crystallins is attributed not only to the presence of hydrophobic residues at interdomain interfaces,[35,36,47] crucial for bringing them in specific orientation, but also to the absence of this serine in vertebrate homologues.

In essence, this work suggests that while ancestors of lens βγ-crystallins may have needed Ca^{2+} for their functions, most of the binding sites in lens βγ-crystallins (and also in paralog non-lens vertebrate members) were disabled to impart domain stability and used to avoid Ca^{2+}-derived loss of domain stability (for a scheme, Figure 9). A deviation or alteration in a domain endowing it with microbial characteristics would lead to compromised transparency of lens leading to premature cataracts, as seen in the case of the R77S mutation in lens γD-crystallin, implicated in juvenile autosomal dominant cataract.[37]

■ ASSOCIATED CONTENT

Ⓢ Supporting Information

Comparisons of domain properties with two-domain proteins, thermal unfolding, quaternary association, and hydrophobicity by bis-ANS, photolability of R77S mutants, and thermodynamic parameters of Ca^{2+} binding to γB-crystallin deduced from ITC. This material is available free of charge via the Internet at http://pubs.acs.org.

■ AUTHOR INFORMATION

Corresponding Author

*Phone: +91-40-27192561. Fax: +91-40-27160591. E-mail: yogendra@ccmb.res.in.

Author Contributions

†S.K.S. and A.M. contributed equally to this work.

Funding

This work was supported by the CSIR 12th five year intramural research grant. S.K.S. and I.D.R. are the recipients of fellowships from the Council of Scientific and Industrial Research and UGC, India, respectively.

Notes

The authors declare no competing financial interest.

■ ACKNOWLEDGMENTS

We thank Syed Sayeed Abdul for his technical help in the laboratory.

■ ABBREVIATIONS

AIM1, absent in melanoma-1; CD, circular dichroism; GdmCl, guanidinium chloride; $c_{1/2}$, midpoint of unfolding transition; NTD, N-terminal domain; CTD, C-terminal domain

■ REFERENCES

(1) Wistow, G. J., and Piatigorsky, J. (1988) Lens crystallins: The evolution and expression of proteins for a highly specialized tissue. *Annu. Rev. Biochem. 57*, 479−504.

(2) Lubsen, N. H., Aarts, H. J., and Schoenmakers, J. G. (1988) The evolution of lenticular proteins: The β- and γ-crystallin super gene family. *Prog. Biophys. Mol. Biol. 51*, 47−76.

(3) Wistow, G. (1990) Evolution of a protein superfamily: Relationships between vertebrate lens crystallins and microorganism dormancy proteins. *J. Mol. Evol. 30*, 140−145.

(4) Kappé, G., Purkiss, A. G., van Genesen, S. T., Slingsby, C., and Lubsen, N. H. (2010) Explosive expansion of βγ-crystallin genes in the ancestral vertebrate. *J. Mol. Evol. 71*, 219−230.

(5) Ray, M. E., Wistow, G., Su, Y. A., Meltzer, P. S., and Trent, J. M. (1997) AIM1, a novel non-lens member of the βγ-crystallin superfamily, is associated with the control of tumorigenicity in human malignant melanoma. *Proc. Natl. Acad. Sci. U.S.A. 94*, 3229−3234.

(6) Aravind, P., Wistow, G., Sharma, Y., and Sankaranarayanan, R. (2008) Exploring the limits of sequence and structure in a variant βγ-crystallin domain of the protein Absent in Melanoma-1 (AIM1). *J. Mol. Biol. 381*, 509−518.
(7) Rajanikanth, V., Srivastava, S. S., Singh, A. K., Rajyalakshmi, M., Chandra, K., Aravind, P., Sankaranarayanan, R., and Sharma, Y. (2012) Aggregation-prone near-native intermediate formation during unfolding of a structurally similar nonlenticular βγ-crystallin domain. *Biochemistry 51*, 8502−8513.
(8) Shimeld, S. M., Purkiss, A. G., Dirks, R. P., Bateman, O. A., Slingsby, C., and Lubsen, N. H. (2005) Urochordate βγ-crystallin and the evolutionary origin of the vertebrate eye lens. *Curr. Biol. 15*, 1684−1689.
(9) Clout, N. J., Kretschmar, M., Jaenicke, R., and Slingsby, C. (2001) Crystal structure of the calcium-loaded spherulin 3a dimer sheds light on the evolution of the eye lens βγ-crystallin domain fold. *Structure (Cambridge, MA, U. S.) 9*, 115−124.
(10) Vergara, A., Grassi, M., Sica, F., Pizzo, E., D'Alessio, G., Mazzarella, L., and Merlino, A. (2013) A novel interdomain interface in crystallins: Structural characterization of the βγ-crystallin from *Geodia cydonium* at 0.99 Å resolution. *Acta Crystallogr. D69*, 960−967.
(11) Wistow, G., Summers, L., and Blundell, T. (1985) *Myxococcus xanthus* spore coat protein S may have a similar structure to vertebrate lens βγ-crystallins. *Nature 315*, 771−773.
(12) Wenk, M., and Mayr, E. M. (1998) *Myxococcus xanthus* spore coat protein S, a stress-induced member of the βγ-crystallin superfamily, gains stability from binding of calcium ions. *Eur. J. Biochem. 255*, 604−610.
(13) Clout, N. J., Slingsby, C., and Wistow, G. J. (1997) An eye on crystallins. *Nat. Struct. Biol. 4*, 685.
(14) Bagby, S., Harvey, T. S., Eagle, S. G., Inouye, S., and Ikura, M. (1994) Structural similarity of a developmentally regulated bacterial spore coat protein to βγ-crystallins of the vertebrate eye lens. *Proc. Natl. Acad. Sci. U.S.A. 91*, 4308−4312.
(15) Jobby, M. K., and Sharma, Y. (2005) Calcium-binding crystallins from *Yersinia pestis*: Characterization of two single βγ-crystallin domains of a putative exported protein. *J. Biol. Chem. 280*, 1209−1216.
(16) Jobby, M. K., and Sharma, Y. (2007) Caulollins from *Caulobacter crescentus*, a pair of partially unstructured proteins of βγ-crystallin superfamily gains structure upon binding calcium. *Biochemistry 46*, 12298−12307.
(17) Aravind, P., Suman, S. K., Mishra, A., Sharma, Y., and Sankaranarayanan, R. (2009) βγ-Crystallin superfamily contains a universal motif for binding calcium. *Biochemistry 48*, 12180−12190.
(18) Barnwal, R. P., Jobby, M. K., Devi, K. M., Sharma, Y., and Chary, K. V. (2009) Solution structure and calcium-binding properties of M-crystallin, a primordial βγ-crystallin from archaea. *J. Mol. Biol. 386*, 675−689.
(19) Bloemendal, H., de Jong, W., Jaenicke, R., Lubsen, N. H., Slingsby, C., and Tardieu, A. (2004) Ageing and vision: Structure, stability and function of lens crystallins. *Prog. Biophys. Mol. Biol. 86*, 407−485.
(20) Suman, S. K., Mishra, A., Ravindra, D., Yeramala, L., and Sharma, Y. (2011) Evolutionary remodelling of the βγ-crystallins for domain stability at cost of Ca^{2+}-binding. *J. Biol. Chem. 286*, 43891−43901.
(21) Rajini, B., Shridas, P., Sundari, C. S., Muralidhar, D., Chandani, S., Thomas, F., and Sharma, Y. (2001) Calcium binding properties of γ-crystallin: Calcium ion binds at the Greek key βγ-crystallin fold. *J. Biol. Chem. 276*, 38464−38471.
(22) Jobby, M. K., and Sharma, Y. (2007) Calcium-binding to lens βB2- and βA3-crystallins suggests that all β-crystallins are calcium-binding proteins. *FEBS J. 274*, 4135−4147.
(23) Ganguly, K., Favor, J., Neuhäuser-Klaus, A., Sandulache, R., Puk, O., Beckers, J., Horsch, M., Schädler, S., Vogt Weisenhorn, D., Wurst, W., and Graw, J. (2008) Novel allele of crybb2 in the mouse and its expression in the brain. *Invest. Ophthalmol. Visual Sci. 49*, 1533−1541.
(24) Xiang, F., Cui, B., Gao, Q., Zhang, J., Zhang, J., and Li, W. (2012) Decreased levels of Ca^{2+}-calmodulin-dependent protein kinase IV in the testis as a contributing factor to reduced fertility in male Crybb2$^{-/-}$ mice. *Int. J. Mol. Med. 30*, 1145−1151.
(25) Teintze, M., Inouye, M., and Inouye, S. (1988) Characterization of calcium-binding sites in development-specific protein S of *Myxococcus xanthus* using site-specific mutagenesis. *J. Biol. Chem. 263*, 1199−1203.
(26) Kretschmar, M., Mayr, E. M., and Jaenicke, R. (1999) Kinetic and thermodynamic stabilization of the βγ-crystallin homolog spherulin 3a from *Physarum polycephalum* by calcium binding. *J. Mol. Biol. 289*, 701−705.
(27) Blundell, T., Lindley, P., Miller, L., Moss, D., Slingsby, C., Tickle, I., Turnell, B., and Wistow, G. (1981) The molecular structure and stability of the eye lens: X-ray analysis of β-crystallin II. *Nature 289*, 771−777.
(28) Wistow, G., Turnell, B., Summers, L., Slingsby, C., Moss, D., Miller, L., Lindley, P., and Blundell, T. (1983) X-ray analysis of the eye lens protein gamma-II crystallin at 1.9 Å resolution. *J. Mol. Biol. 170*, 175−202.
(29) Mishra, A., Suman, S. K., Srivastava, S. S., Sankaranarayanan, R., and Sharma, Y. (2012) Decoding the molecular design principles underlying Ca^{2+}-binding to βγ-crystallin motifs. *J. Mol. Biol. 415*, 75−91.
(30) Ji, F., Jung, J., and Gronenborn, A. M. (2012) Structural and biochemical characterization of the childhood cataract-associated R76S mutant of human γD-crystallin. *Biochemistry 51*, 2588−2596.
(31) Pace, C. N. (1986) Determination and analysis of urea and guanidine hydrochloride denaturation curves. *Methods Enzymol. 131*, 266−280.
(32) Nobuhiko, T., and Tawfik, D. S. (2009) Stability effects of mutations and protein evolvability. *Curr. Opin. Struct. Biol. 19*, 596−604.
(33) Chen, J., Callis, P. R., and King, J. (2009) Mechanism of the very efficient quenching of tryptophan fluorescence in human γD- and γS-crystallins: The γ-crystallin fold may have evolved to protect tryptophan residues from ultraviolet photo-damage. *Biochemistry 48*, 3708−3716.
(34) Rajini, B., Graham, C., Wistow, G., and Sharma, Y. (2003) Stability, homodimerization, and calcium-binding properties of a single, variant βγ-crystallin domain of the protein absent in melanoma 1 (AIM1). *Biochemistry 42*, 4552−4559.
(35) Flaugh, S. L., Kosinski-Collins, M. S., and King, J. (2005) Contributions of hydrophobic domain interface interactions to the folding and stability of human γD-crystallin. *Protein Sci. 14*, 569−581.
(36) Moreau, K. L., and King, J. (2009) Hydrophobic core mutations associated with cataract development in mice destabilize human γD-crystallin. *J. Biol. Chem. 284*, 33285−33295.
(37) Roshan, M., Vijaya, P. H., Lavanya, G. R., Shama, P. K., Santhiya, S. T., Graw, J., Gopinath, P. M., and Satyamoorthy, K. (2010) A novel human CRYGD mutation in a juvenile autosomal dominant cataract. *Mol. Vis. 16*, 887−896.
(38) Clark, J. I., Mengel, L., Bagg, A., and Benedek, G. B. (1981) Cortical opacity, calcium concentration and fiber membrane structure in the calf lens. *Exp. Eye Res. 31*, 399−410.
(39) Duncan, G., and Jacob, T. J. (1984) Influence of external calcium and glucose on internal total and ionized calcium in the rat lens. *J. Physiol. 357*, 485−493.
(40) Vrensen, G. F., Sanderson, J., Willekens, B., and Duncan, G. (1995) Calcium localization and ultrastructure of clear and pCMPS-treated rat lenses. *Invest. Ophthalmol. Visual Sci. 36*, 2287−2295.
(41) Rhodes, J. D., Collison, D. J., and Duncan, G. (2003) Calcium activates SK channels in the intact human lens. *Invest. Ophthalmol. Visual Sci. 44*, 3927−39232.
(42) Rhodes, J. D., and Sanderson, J. (2009) The mechanisms of calcium homeostasis and signaling in the lens. *Exp. Eye Res. 88*, 226−234.
(43) Baruch, A., Greenbaum, D., Levy, E. T., Nielsen, P. A., Gilula, N. B., Kumar, N. M., and Bogyo, M. (2001) Defining a link between gap junction communication, proteolysis, and cataract formation. *J. Biol. Chem. 276*, 28999−29006.

(44) Gao, J., Sun, X., Martinez-Wittinghan, F. J., Gong, X., White, T. W., and Mathias, R. T. (2004) Connections between connexins, calcium, and cataracts in the lens. *J. Gen. Physiol. 124*, 289−300.
(45) Clemens, D. M., Németh-Cahalan, K. L., Trinh, L., Zhang, T., Schilling, T. F., and Hall, J. E. (2013) In vivo analysis of aquaporin 0 function in zebrafish: Permeability regulation is required for lens transparency. *Invest. Ophthalmol. Visual Sci. 54*, 5136−5143.
(46) Maddala, R., Nagendran, T., de Ridder, G. G., Schey, K. L., and Rao, P. V. (2013) L-type calcium channels play a critical role in maintaining lens transparency by regulating phosphorylation of aquaporin-0 and myosin light chain and expression of connexins. *PLoS One 8*, No. e64676.
(47) Das, P., King, J. A., and Zhou, R. (2011) Aggregation of γ-crystallins associated with human cataracts via domain swapping at the C-terminal β-strands. *Proc. Natl. Acad. Sci. U.S.A. 108*, 10514−10519.